Diffractive Deep Inelastic Scattering in the Dipole Picture at Next-to-Leading Order

Henri Hänninen

Centre of Excellence in Quark Matter,
University of Jyväskylä, Finland

Centre of Excellence of Inverse Modelling and Imaging,
University of Jyväskylä, Finland

In collaboration with
G. Beuf, T. Lappi, Y. Mulian, H. Mäntysaari

ACADEMY OF FINLAND

CENTRES OF EXCELLENCE IN RESEARCH

e-Print: **2206.13161 [hep-ph]**

DIS2023, Michigan, USA

March 29, 2023

Diffractive scattering of particles

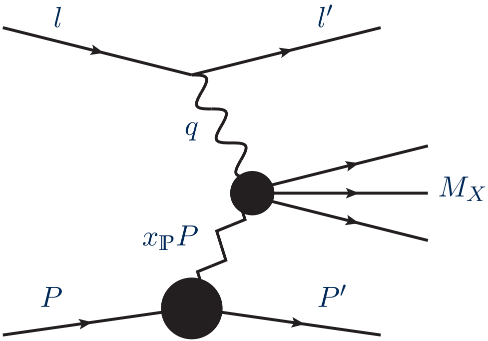

Inclusive lepton–proton diffractive scattering

- Virtual photon γ^* scatters off the target without exchanging color-charge.

Diffractive scattering of particles

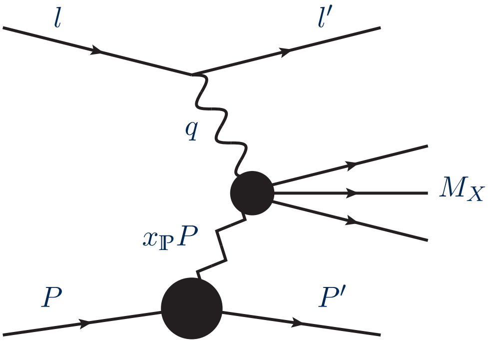

Inclusive lepton–proton diffractive scattering

- Virtual photon γ^* scatters off the target without exchanging color-charge.
- γ^* remnants form a diffractive final state of invariant mass M_X.

Diffractive scattering of particles

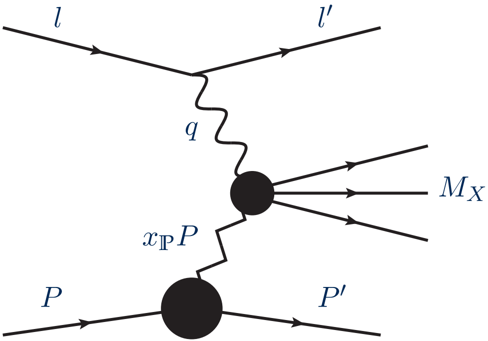

Inclusive lepton–proton diffractive scattering

- Virtual photon γ^* scatters off the target without exchanging color-charge.
- γ^* remnants form a diffractive final state of invariant mass M_X.
- A sizable gap between the outgoing proton and diffractive systems is seen.
  - Gap size $\Delta y \sim \log \frac{1}{x_{\mathbb{P}}}$.
  - $x_{\mathbb{P}} = \frac{x_{Bj}}{\beta}$, $\beta = \frac{Q^2}{Q^2+M_X^2}$.

Diffractive scattering of particles

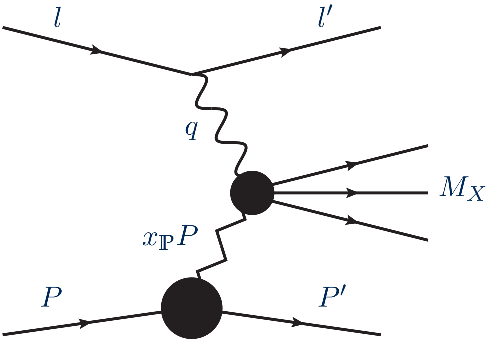

Inclusive lepton–proton diffractive scattering

- Virtual photon γ^* scatters off the target without exchanging color-charge.
- γ^* remnants form a diffractive final state of invariant mass M_X.
- A sizable gap between the outgoing proton and diffractive systems is seen.
  - Gap size $\Delta y \sim \log \frac{1}{x_{\mathbb{P}}}$.
  - $x_{\mathbb{P}} = \frac{x_{Bj}}{\beta}, \ \beta = \frac{Q^2}{Q^2+M_X^2}$.
- A substantial proportion $(10-15\%)$ of all *ep*-collisions seen at HERA were diffractive, whereas a simple QCD expectation is that large-gap events would be exponentially suppressed.[a]

[a] Bjorken, Phys. Rev. D 47 (1993) 101

Diffractive DIS in the Dipole Picture

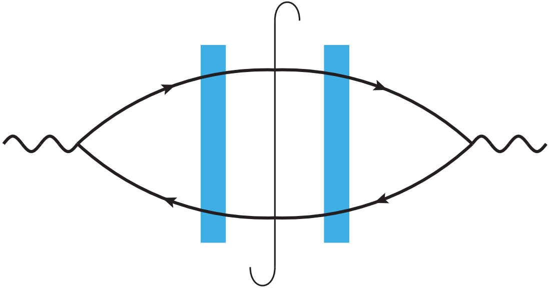

Scattering amplitude squared of leading order diffractive $\gamma^* p$ scattering. Produced color-singlet $q\bar{q}$ pair forms the diffractive state of invariant mass M_X at a large separation from the outgoing target.

Diffractive DIS in the Dipole Picture

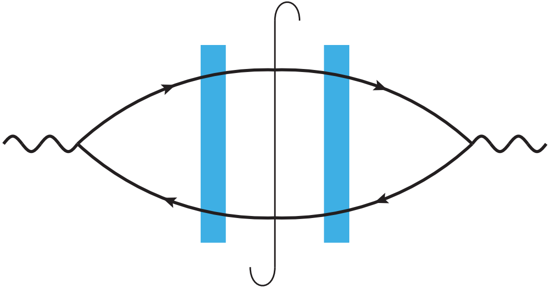

Scattering amplitude squared of leading order diffractive $\gamma^* p$ scattering. Produced color-singlet $q\bar{q}$ pair forms the diffractive state of invariant mass M_X at a large separation from the outgoing target.

Inclusive diffractive cross section in the dipole picture is:

$$\frac{\mathrm{d}\sigma^{\mathrm{D}}_{\lambda,\, q\bar{q}}}{\mathrm{d}M_X^2\,\mathrm{d}|t|} = \frac{N_\mathrm{c}}{4\pi}\int_0^1 \mathrm{d}z \int_{\mathbf{x}_0\mathbf{x}_1\bar{\mathbf{x}}_0\bar{\mathbf{x}}_1} \mathcal{I}^{(2)}_{\boldsymbol{\Delta}}\mathcal{I}^{(2)}_{M_X}\sum_f\sum_{h_0,h_1}\left(\widetilde{\psi}_{\gamma^*_\lambda\to q_{\bar{0}}\bar{q}_{\bar{1}}}\right)^\dagger\left(\widetilde{\psi}_{\gamma^*_\lambda\to q_0\bar{q}_1}\right)\left[S^\dagger_{\bar{0}\bar{1}}-1\right]\left[S_{01}-1\right],$$

$$\mathcal{I}^{(2)}_{M_X} = \frac{1}{4\pi}\mathrm{J}_0\left(\sqrt{z_0 z_1}M_X\|\bar{\mathbf{r}}-\mathbf{r}\|\right), \qquad \mathcal{I}^{(2)}_{\boldsymbol{\Delta}} = \frac{1}{4\pi}\mathrm{J}_0\left(\sqrt{|t|}\left\|\bar{\mathbf{b}}-\mathbf{b}+\frac{(2z_0-1)}{2}(\bar{\mathbf{r}}-\mathbf{r})\right\|\right).$$

Observation of DDIS at HERA

Why was the LO dipole picture result insufficient to describe diffractive HERA data?

Observation of DDIS at HERA

Why was the LO dipole picture result insufficient to describe diffractive HERA data?

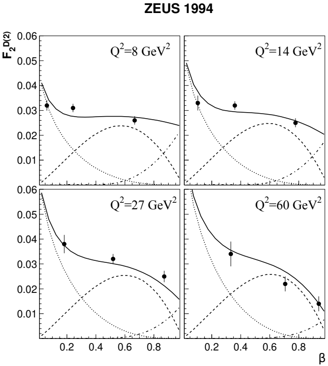

Golec-Biernat, Wusthoff, Phys.Rev.D 60 (1999) 114023, hep-ph/9903358 [hep-ph]

- Longitudinal $q\bar{q}$ dominates F_2^{D} at $\beta \sim 1$
- Transverse $q\bar{q}$ dominates F_2^{D} at $\beta \sim 0.5$, i.e. $M_X^2 \sim Q^2$
- Transverse $q\bar{q}g$ becomes important at $\beta \to 0$.

Observation of DDIS at HERA

Why was the LO dipole picture result insufficient to describe diffractive HERA data?

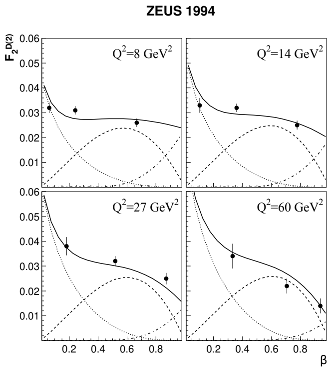

Golec-Biernat, Wusthoff, Phys.Rev.D 60 (1999) 114023, hep-ph/9903358 [hep-ph]

- Longitudinal $q\bar{q}$ dominates F_2^{D} at $\beta \sim 1$
- Transverse $q\bar{q}$ dominates F_2^{D} at $\beta \sim 0.5$, i.e. $M_X^2 \sim Q^2$
- Transverse $q\bar{q}g$ becomes important at $\beta \to 0$.

$\Rightarrow$ A number of pioneering analyses calculated the $q\bar{q}g$ contribution to F_T^{D} under varying assumptions or approximations. Bartels:1999, Kovchegov:1999, Kopeliovich:1999, Kovchegov:2001, Munier:2003, Golec-Biernat:2005, Wusthoff:1997, GolecBiernat:1999, GolecBiernat:2001

The $q\bar{q}g$-contribution at Next-to-Leading Order

Tree-level diagrams

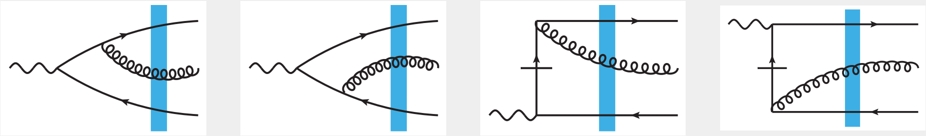

- $\widetilde{\psi}_{\gamma^*_\lambda \to q_0 \bar{q}_1 g_2}$ splitting wavefunction calculated in arXiv:1708.06557, arXiv:1711.08207
  $\Rightarrow \mathrm{d}\sigma^{\mathrm{D}} \sim \mathcal{M}^\dagger \mathcal{M} \sim \widetilde{\psi}^\dagger_{\gamma^*_\lambda \to q_0 \bar{q}_1 g_2} \widetilde{\psi}_{\gamma^*_\lambda \to q_0 \bar{q}_1 g_2}$
- Constraint on final state M_X makes these contributions finite by themselves
  $\Rightarrow$ reasonable finite subset of the full NLO contribution that supersedes approximative results in the literature.
- New results involve full 3-particle phase space $(\mathbf{x}_0, \mathbf{x}_1, \mathbf{x}_2, \overline{\mathbf{x}}_0, \overline{\mathbf{x}}_1, \overline{\mathbf{x}}_2)$, final state transfer functions $\mathcal{I}^{(3)}_{M_X}$, $\mathcal{I}^{(3)}_{\boldsymbol{\Delta}}$, and explicit squared splitting wavefunctions.

3-particle final state phase space

- Final state production phase does not care about the producing diagram.
  - It is fully determined by the number of Fock state constituents.
- Producing a final state of mass M_X:

$$\mathcal{I}_{M_X}^{(3)} = 2\frac{z_0 z_1 z_2}{(4\pi)^2}\frac{M_X}{Y_{012}} \mathrm{J}_1\left(M_X Y_{012}\right),$$

with

$$\mathbf{Y}_{012}^2 = z_0 z_1 \left(\mathbf{x}_{\bar{0}0} - \mathbf{x}_{\bar{1}1}\right)^2 + z_1 z_2 \left(\mathbf{x}_{\bar{2}2} - \mathbf{x}_{\bar{1}1}\right)^2 + z_0 z_2 \left(\mathbf{x}_{\bar{2}2} - \mathbf{x}_{\bar{0}0}\right)^2.$$

- Momentum transfer dependence factorizes:

$$\mathcal{I}_{\mathbf{\Delta}}^{(3)} = \frac{1}{4\pi}\mathrm{J}_0\left(\sqrt{-t}\|z_0\mathbf{x}_{\bar{0}0} + z_1\mathbf{x}_{\bar{1}1} + z_2\mathbf{x}_{\bar{2}2}\|\right).$$

$q\bar{q}g$-contribution: longitudinal (New)

$$x_{\mathbb{P}} F^{\mathrm{D}(4)\,\mathrm{NLO}}_{L,\,q\bar{q}g}(x_{Bj}, Q^2, \beta, t) = 4\frac{\alpha_{\mathrm{s}} N_{\mathrm{c}} C_{\mathrm{F}} Q^4}{\beta} \sum_f e_f^2 \int_0^1 \frac{\mathrm{d}z_0}{z_0} \int_0^1 \frac{\mathrm{d}z_1}{z_1} \int_0^1 \frac{\mathrm{d}z_2}{z_2} \delta(z_0+z_1+z_2-1)$$

$$\times \int_{\mathbf{x}_0} \int_{\mathbf{x}_1} \int_{\mathbf{x}_2} \int_{\overline{\mathbf{x}}_0} \int_{\overline{\mathbf{x}}_1} \int_{\overline{\mathbf{x}}_2} \mathcal{I}^{(3)}_{M_X} \mathcal{I}^{(3)}_{\boldsymbol{\Delta}}\, 4 z_0 z_1 Q^2 \mathrm{K}_0\left(Q X_{012}\right) \mathrm{K}_0\left(Q X_{\overline{0}\,\overline{1}\,\overline{2}}\right)$$

$$\times \Bigg\{ z_1^2 \Bigg[\left(2z_0(z_0+z_2)+z_2^2\right) \left(\frac{\mathbf{x}_{20}}{\mathbf{x}_{20}^2} \cdot \left(\frac{\mathbf{x}_{\overline{2}\,\overline{0}}}{\mathbf{x}_{\overline{2}\,\overline{0}}^2} - \frac{1}{2} \frac{\mathbf{x}_{\overline{2}\,\overline{1}}}{\mathbf{x}_{\overline{2}\,\overline{1}}^2} \right) - \frac{1}{2} \frac{\mathbf{x}_{\overline{2}\,\overline{0}} \cdot \mathbf{x}_{21}}{\mathbf{x}_{\overline{2}\,\overline{0}}^2 \mathbf{x}_{21}^2} \right) + \frac{z_2^2}{2} \left(\frac{\mathbf{x}_{\overline{2}\,\overline{0}} \cdot \mathbf{x}_{21}}{\mathbf{x}_{\overline{2}\,\overline{0}}^2 \mathbf{x}_{21}^2} + \frac{\mathbf{x}_{20} \cdot \mathbf{x}_{\overline{2}\,\overline{1}}}{\mathbf{x}_{20}^2 \mathbf{x}_{\overline{2}\,\overline{1}}^2} \right) \Bigg]$$

$$+ z_0^2 \Bigg[\left(2z_1(z_1+z_2)+z_2^2\right) \left(\frac{\mathbf{x}_{21}}{\mathbf{x}_{21}^2} \cdot \left(\frac{\mathbf{x}_{\overline{2}\,\overline{1}}}{\mathbf{x}_{\overline{2}\,\overline{1}}^2} - \frac{1}{2} \frac{\mathbf{x}_{\overline{2}\,\overline{0}}}{\mathbf{x}_{\overline{2}\,\overline{0}}^2} \right) - \frac{1}{2} \frac{\mathbf{x}_{20} \cdot \mathbf{x}_{\overline{2}\,\overline{1}}}{\mathbf{x}_{20}^2 \mathbf{x}_{\overline{2}\,\overline{1}}^2} \right) + \frac{z_2^2}{2} \left(\frac{\mathbf{x}_{\overline{2}\,\overline{0}} \cdot \mathbf{x}_{21}}{\mathbf{x}_{\overline{2}\,\overline{0}}^2 \mathbf{x}_{21}^2} + \frac{\mathbf{x}_{20} \cdot \mathbf{x}_{\overline{2}\,\overline{1}}}{\mathbf{x}_{20}^2 \mathbf{x}_{\overline{2}\,\overline{1}}^2} \right) \Bigg] \Bigg\}$$

$$\times \left[1 - S^{\dagger}_{\overline{0}\,\overline{1}\,\overline{2}}\right] \left[1 - S_{012}\right],$$

- Not known previously in the literature.

$q\bar{q}g$-contribution: transverse (New)

$$x_{\mathbb{P}} F_{T,\, q\bar{q}g}^{\mathrm{D}(4)\,\mathrm{NLO}}(x_{Bj}, Q^2, \beta, t) = 2\frac{\alpha_{\mathrm{s}} N_{\mathrm{c}} C_{\mathrm{F}} Q^4}{\beta} \sum_f e_f^2 \int_0^1 \frac{\mathrm{d}z_0}{z_0} \int_0^1 \frac{\mathrm{d}z_1}{z_1} \int_0^1 \frac{\mathrm{d}z_2}{z_2} \delta(z_0+z_1+z_2-1) \int_{\substack{\mathbf{x}_0, \mathbf{x}_1, \mathbf{x}_2, \\ \overline{\mathbf{x}}_0, \overline{\mathbf{x}}_1, \overline{\mathbf{x}}_2}} \mathcal{I}_{M_X}^{(3)} \mathcal{I}_{\mathbf{\Delta}}^{(3)}$$

$$\times \frac{z_0 z_1 Q^2}{X_{012} X_{\overline{0}\,\overline{1}\,\overline{2}}} \mathrm{K}_1\left(Q X_{012}\right) \mathrm{K}_1\left(Q X_{\overline{0}\,\overline{1}\,\overline{2}}\right) \left\{ \Upsilon_{\mathrm{reg.}}^{(|b|^2)} + \Upsilon_{\mathrm{reg.}}^{(|c|^2)} + \Upsilon_{\mathrm{inst.}}^{d} + \Upsilon_{\mathrm{inst.}}^{e} + \Upsilon_{\mathrm{interf.}}^{b\times c} \right\} \left[1 - S_{\overline{0}\,\overline{1}\,\overline{2}}^{\dagger}\right] \left[1 - S_{012}\right],$$

$$\begin{aligned}
\Upsilon_{\mathrm{reg.}}^{(|b|^2)} = {} & z_1^2 \Bigg[(2 z_0 (z_0 + z_2) + z_2^2)(1 - 2 z_1 (1 - z_1)) \left(\mathbf{x}_{\overline{0}+\overline{2};\overline{1}} \cdot \mathbf{x}_{0+2;1} \right) \frac{(\mathbf{x}_{\overline{2}\,\overline{0}} \cdot \mathbf{x}_{20})}{\mathbf{x}_{\overline{2}\,\overline{0}}^2 \mathbf{x}_{20}^2} \\
& - z_2 (2 z_0 + z_2)(2 z_1 - 1) \frac{\left(\mathbf{x}_{\overline{0}+\overline{2};\overline{1}} \cdot \mathbf{x}_{\overline{2}\,\overline{0}} \right) \left(\mathbf{x}_{0+2;1} \cdot \mathbf{x}_{20} \right) - \left(\mathbf{x}_{\overline{0}+\overline{2};\overline{1}} \cdot \mathbf{x}_{20} \right) \left(\mathbf{x}_{0+2;1} \cdot \mathbf{x}_{\overline{2}\,\overline{0}} \right)}{\mathbf{x}_{\overline{2}\,\overline{0}}^2 \mathbf{x}_{20}^2} \Bigg],
\end{aligned}$$

$$\Upsilon_{\mathrm{inst.}}^{d} = \frac{z_0^2 z_1^2 z_2^2}{(z_0 + z_2)^2} - \frac{z_0^2 z_1^3 z_2}{z_0 + z_2} \left(\frac{\mathbf{x}_{0+2;1} \cdot \mathbf{x}_{20}}{\mathbf{x}_{20}^2} + \frac{\mathbf{x}_{\overline{0}+\overline{2};\overline{1}} \cdot \mathbf{x}_{\overline{2}\,\overline{0}}}{\mathbf{x}_{\overline{2}\,\overline{0}}^2} \right) + \frac{z_0^2 z_1 (z_1 + z_2)^2 z_2}{z_0 + z_2} \left(\frac{\mathbf{x}_{0;1+2} \cdot \mathbf{x}_{21}}{\mathbf{x}_{21}^2} + \frac{\mathbf{x}_{\overline{0};\overline{1}+\overline{2}} \cdot \mathbf{x}_{\overline{2}\,\overline{1}}}{\mathbf{x}_{\overline{2}\,\overline{1}}^2} \right),$$

$$\begin{aligned}
\Upsilon_{\mathrm{interf.}}^{b\times c} = {} & - z_0 z_1 \left[z_1 (z_0 + z_2) + z_0 (z_1 + z_2) \right] \left[z_0 (z_0 + z_2) + z_1 (z_1 + z_2) \right] \left[\left(\mathbf{x}_{\overline{0}+\overline{2};\overline{1}} \cdot \mathbf{x}_{0;1+2} \right) \frac{(\mathbf{x}_{\overline{2}\,\overline{0}} \cdot \mathbf{x}_{21})}{\mathbf{x}_{\overline{2}\,\overline{0}}^2 \mathbf{x}_{21}^2} + \left(\mathbf{x}_{\overline{0};\overline{1}+\overline{2}} \cdot \mathbf{x}_{0+2;1} \right) \frac{(\mathbf{x}_{\overline{2}\,\overline{1}} \cdot \mathbf{x}_{20})}{\mathbf{x}_{\overline{2}\,\overline{1}}^2 \mathbf{x}_{20}^2} \right] + z_0 z_1 z_2 (z_0 - z_1)^2 \\
& \times \left[\frac{\left(\mathbf{x}_{\overline{0}+\overline{2};\overline{1}} \cdot \mathbf{x}_{\overline{2}\,\overline{0}} \right) \left(\mathbf{x}_{0;1+2} \cdot \mathbf{x}_{21} \right) - \left(\mathbf{x}_{\overline{0}+\overline{2};\overline{1}} \cdot \mathbf{x}_{21} \right) \left(\mathbf{x}_{0;1+2} \cdot \mathbf{x}_{\overline{2}\,\overline{0}} \right)}{\mathbf{x}_{\overline{2}\,\overline{0}}^2 \mathbf{x}_{21}^2} + \frac{\left(\mathbf{x}_{\overline{0};\overline{1}+\overline{2}} \cdot \mathbf{x}_{\overline{2}\,\overline{1}} \right) \left(\mathbf{x}_{0+2;1} \cdot \mathbf{x}_{20} \right) - \left(\mathbf{x}_{\overline{0};\overline{1}+\overline{2}} \cdot \mathbf{x}_{20} \right) \left(\mathbf{x}_{0+2;1} \cdot \mathbf{x}_{\overline{2}\,\overline{1}} \right)}{\mathbf{x}_{\overline{2}\,\overline{1}}^2 \mathbf{x}_{20}^2} \right],
\end{aligned}$$

with diags. $b \leftrightarrow c$ and $d \leftrightarrow e$ related by $q \leftrightarrow \bar{q}$ exchange. First result derived in "exact eikonal kinematics".

Final state emissions contribute to $q\bar{q}g$ production

Tree-level diagrams that are not included in present results

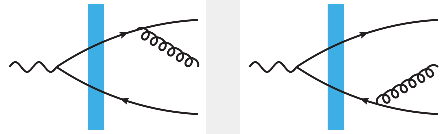

- The $q\bar{q}g$ final state can be produced as a final state emission of a gluon.
- These must be included with the virtual corrections, as they contain a collinear divergence, which is canceled by wavefunction renormalization.[1]

[1] The renormalization correction is also UV divergent which cancels against other 1-loop diagrams.

Future work: 1-loop corrections

1-loop corrections needed for full NLO accuracy:

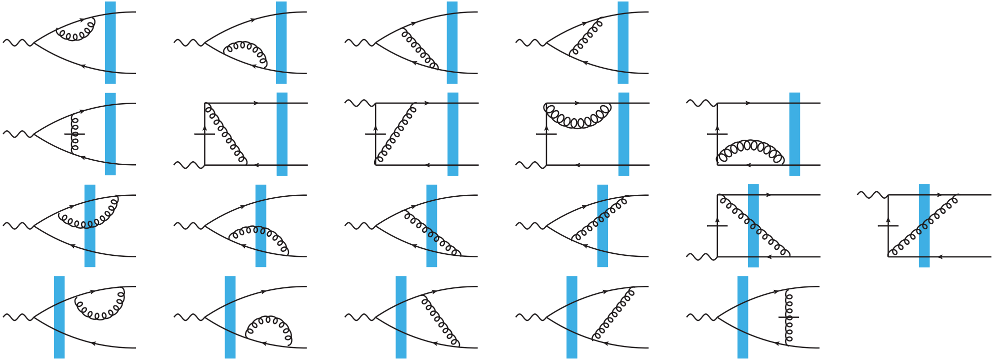

See talk by **J. Penttala**

Recovering known results for F_T^{D}

- Our full NLO result for the $q\bar{q}g$-contribution to F_T^{D} should encompass previous dipole picture results that have used various approximations:
  - Large-M_X, or equivalently small-β, limit[2]
  - Large-Q^2 limit[3]

[2] Inspirehep: Bartels:1999tn, Kovchegov:1999ji, Kopeliovich:1999am, Kovchegov:2001ni, Munier:2003zb, Golec-Biernat:2005prq
[3] Inspirehep: Wusthoff:1997fz, GolecBiernat:1999qd, GolecBiernat:2001mm

Large-M_X limit $q\bar{q}g$-contribution

$$x_{\mathbb{P}} F^{\mathrm{D}\ (\mathrm{MS})}_{T,q\bar{q}g}(x_{\mathbb{P}}, \beta = 0, Q^2) = \frac{\alpha_{\mathrm{s}} N_{\mathrm{c}} C_F Q^2}{16\pi^5 \alpha_{\mathrm{em}}} \int \mathrm{d}^2\mathbf{x}_0 \int \mathrm{d}^2\mathbf{x}_1 \int \mathrm{d}^2\mathbf{x}_2 \int_0^1 \frac{\mathrm{d}z}{z(1-z)} \left| \widetilde{\psi}^{\mathrm{LO}}_{\gamma^*_\lambda \to q_{\bar{0}} \bar{q}_{\bar{1}}} \right|^2$$
$$\times \frac{\mathbf{x}_{01}^2}{\mathbf{x}_{02}^2 \mathbf{x}_{12}^2} \left[N_{02} + N_{12} - N_{01} - N_{02} N_{12} \right]^2 .$$

- Originally derived at the soft gluon emission limit, i.e. $z_2 \to 0$.
- Produces large $M_X^2 \sim \frac{1}{z_2}$.

Large-M_X limit $q\bar{q}g$-contribution

$$x_{\mathbb{P}} F_{T,q\bar{q}g}^{\mathrm{D}\ (\mathrm{MS})}(x_{\mathbb{P}}, \beta = 0, Q^2) = \frac{\alpha_{\mathrm{s}} N_{\mathrm{c}} C_F Q^2}{16\pi^5 \alpha_{\mathrm{em}}} \int \mathrm{d}^2\mathbf{x}_0 \int \mathrm{d}^2\mathbf{x}_1 \int \mathrm{d}^2\mathbf{x}_2 \int_0^1 \frac{\mathrm{d}z}{z(1-z)} \left| \widetilde{\psi}^{\mathrm{LO}}_{\gamma^*_\lambda \to q_0 \bar{q}_1} \right|^2 \times \frac{\mathbf{x}_{01}^2}{\mathbf{x}_{02}^2 \mathbf{x}_{12}^2} \left[N_{02} + N_{12} - N_{01} - N_{02}N_{12} \right]^2 .$$

- Originally derived at the soft gluon emission limit, i.e. $z_2 \to 0$.
- Produces large $M_X^2 \sim \frac{1}{z_2}$.
- We recover this exactly from the full result by:
  - Approximate $z_2 \to 0$, simplifies NLO LCWF structure substantially.
  - Eliminate cross-section M_X dependence via $\int \mathrm{d}z_2 \delta(M_X^2 - \frac{\mathbf{p}_2^2}{z_2})$.
  - Include final state gluon emission contribution to cancel out divergence caused by approximations.

Large-Q^2 limit $q\bar{q}g$-contribution

$$x_{\mathbb{P}} F_{T,q\bar{q}g}^{\mathrm{D\,(GBW)}}\left(x_{\mathbb{P}}, \beta, Q^2\right) = \frac{\alpha_s \beta}{8\pi^4} \sum_f e_f^2 \int \mathrm{d}^2\mathbf{b} \int_0^{Q^2} \mathrm{d}k^2 \int_\beta^1 \mathrm{d}z \Bigg\{ k^4 \ln\frac{Q^2}{k^2} \left[\left(1-\frac{\beta}{z}\right)^2 + \left(\frac{\beta}{z}\right)^2\right]$$
$$\times \left[\int_0^\infty \mathrm{d}r\, r \frac{\mathrm{d}\tilde{\sigma}_{\mathrm{dip}}}{\mathrm{d}^2\mathbf{b}}(\mathbf{b}, \mathbf{r}, x_{\mathbb{P}}) \mathrm{K}_2\left(\sqrt{z}kr\right) \mathrm{J}_2\left(\sqrt{1-z}kr\right)\right]^2 \Bigg\},$$

- Explicit large $\log Q^2$.
- DGLAP $g \to q\bar{q}$ splitting function.
- Postulated “effective gluon wavefunction” results in $\mathrm{K}_2, \mathrm{J}_2$.
- Originally derived in a picture where:
  - Color-singlet $q\bar{q}$ too small to resolve: behaves as an “effective gluon”.
  - Gluon dipole scattered off the target via a two-gluon exchange — later phenomenologically replaced with the dipole scattering amplitude prescription.

Recovering the large-Q^2 limit

- Making kinematic approximations requires a Fourier transform into momentum space.
  - Express light-cone wavefunctions using natural momenta, which are better compatible with the approximations to be done.

- Take the aligned jet limit in the full $q\bar{q}g$ contribution:
  - $z_0 \gg z_1 \gg z_2$
  - $Q^2 \gg \mathbf{P}_{q\bar{q}}^2 \gg \mathbf{K}_{g\tilde{g}}^2 \gg \boldsymbol{\Delta}^2$
  - As $q\bar{q}$-pair too small to resolve: $\mathbf{P}_{q\bar{q}}$ not changed by the shockwave.
  - Integrate out 28 of 34 degrees of freedom $\Rightarrow$ complexity is drastically reduced.

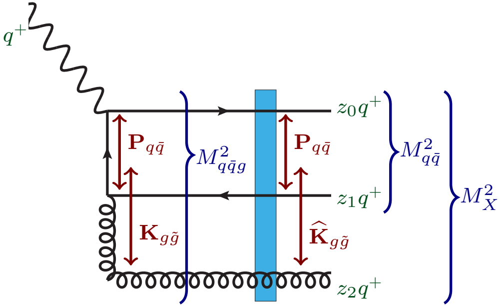

Translating between different physical pictures

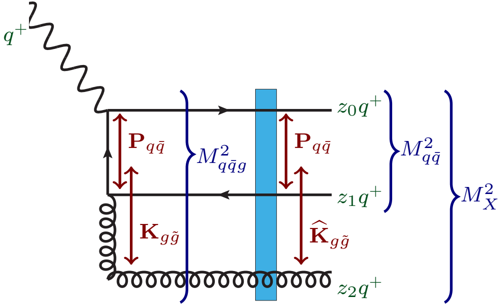

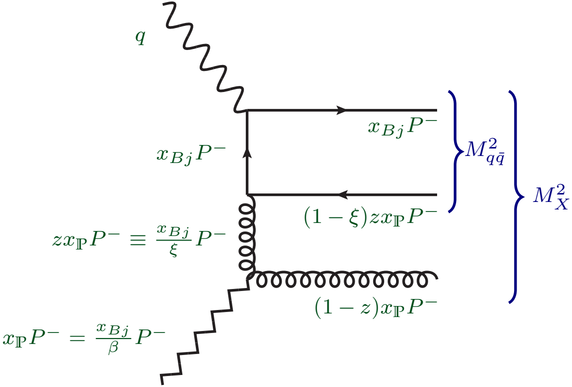

- Translate problem into minus-momentum parametrization by connecting the pictures via invariant masses.

Conclusions

- The first NLO accuracy calculation of the $q\bar{q}g$-contribution to $F^{\mathrm{D}}_{T,L}$ without kinematical approximations, and first calculation of $F^{\mathrm{D}}_{L,\,q\bar{q}g}$ altogether.

Conclusions

- The first NLO accuracy calculation of the $q\bar{q}g$-contribution to $F_{T,L}^{\mathrm{D}}$ without kinematical approximations, and first calculation of $F_{L,\,q\bar{q}g}^{\mathrm{D}}$ altogether.
- As a verification, we recovered two well-known limiting results from the literature.
  - Remarkably, the large-Q^2 collinear factorization of F_T^{D} was found to emerge from the dipole picture. (*a priori*, dipole picture is valid in a different kinematical regime.)
  - Explicit result for the large-Q^2 $q\bar{q}g$-contribution from first principles.

Conclusions

- The first NLO accuracy calculation of the $q\bar{q}g$-contribution to $F^{\mathrm{D}}_{T,L}$ without kinematical approximations, and first calculation of $F^{\mathrm{D}}_{L,\,q\bar{q}g}$ altogether.
- As a verification, we recovered two well-known limiting results from the literature.
  - Remarkably, the large-Q^2 collinear factorization of F^{D}_{T} was found to emerge from the dipole picture. (*a priori*, dipole picture is valid in a different kinematical regime.)
  - Explicit result for the large-Q^2 $q\bar{q}g$-contribution from first principles.
- In the future:
  - Calculation of all the 1-loop diagrams. (talk by J. Penttala)
  - Numerical implementation of the $q\bar{q}g$-contribution. (WIP)
  - Global analysis of structure function and vector meson data in the dipole picture.

Conclusions

- The first NLO accuracy calculation of the $q\bar{q}g$-contribution to $F^{\mathrm{D}}_{T,L}$ without kinematical approximations, and first calculation of $F^{\mathrm{D}}_{L,\,q\bar{q}g}$ altogether.
- As a verification, we recovered two well-known limiting results from the literature.
  - Remarkably, the large-Q^2 collinear factorization of F^{D}_{T} was found to emerge from the dipole picture. (*a priori*, dipole picture is valid in a different kinematical regime.)
  - Explicit result for the large-Q^2 $q\bar{q}g$-contribution from first principles.
- In the future:
  - Calculation of all the 1-loop diagrams. (talk by J. Penttala)
  - Numerical implementation of the $q\bar{q}g$-contribution. (WIP)
  - Global analysis of structure function and vector meson data in the dipole picture.

Thank you for your attention.